Geoscience Laser Altimeter System (GLAS)

Algorithm Theoretical Basis Document
Version 1.0

ATMOSPHERIC DELAY CORRECTION TO GLAS LASER ALTIMETER RANGES

Prepared by:

T. A. Herring
K. Quinn
Massachusetts Institute of Technology
Cambridge, MA

February 1999

Table of Contents

1.0 Introduction

The ICESat (Ice, Cloud, and Land Elevation Satellite) mission will be launched July 2001. This mission will use the GLAS (Geoscience Laser Altimeter System) instrument to determine the topography of the polar ice sheets. To accurately measure the ranges it is necessary to correct for the atmospheric delay of the laser pulses. Atmospheric delay depends on the refractive index along the path that the laser pulse takes through the atmosphere. The refractive index of air at optical wavelengths is a function of density. For ray paths near zenith the atmospheric delay can be shown to be almost directly related to surface pressure and total column precipitable water vapor, the deviation being due to variations of gravity with respect to height and the effects of non-hydrostatic forces in the atmosphere. For ray paths off zenith a mapping function relates the delay to the zenith delay.

Values for surface pressure and precipitable water vapor will be calculated from global atmospheric analyses. We use the NCEP Global Analyses, a 1 by 1 degree gridded data set with sampling every 6 hours. Variables included are temperature, geopotential height and relative humidity at standard upper atmospheric pressure levels. These atmospheric fields are interpolated to the location and time tag of the laser footprints.

Note that all units used in the following text are SI unless otherwise stated.

2.0 Algorithm Description

2.1 Atmospheric Range Correction Model

The one-way correction to the GLAS range measurement, ΔL, due the refractive effects of the Earth's atmosphere is defined as

$$\Delta L = \int_{Satm} n(s)ds - \int_{Svac} ds \tag{1.1}$$

where *n(s)* is the refractive index of the atmosphere along the ray path, *Satm* is the curved path followed by the laser pulse from the space craft to the ground, and *Svac* is the straight line path from the space craft to the ground. Evaluation of the second integral only requires the space craft and laser footprint coordinates. Evaluation of the first integral also requires knowledge of the refractive index along the ray path and is most accurately calculated using ray tracing or numerical integration methods. Direct ray tracing is not practical for large amounts of data, however semi-analytical models can provide results that deviate near zenith from ray tracing by < 1mm. Models that relate the total delay to the zenith delay by a mapping function are commonly used such that

$$\Delta L = m(\varepsilon, \boldsymbol{P}) \int_{Z}^{\infty} (n(z) - 1)dz \tag{1.2}$$

where $m(\varepsilon, \boldsymbol{P})$ is a mapping function that depends on elevation angle, ε, and a parameter vector

P. The integral is evaluated along a zenith path from ground point, *Z*, to the space craft. The mapping function will be described in section 2.2.

The argument of the integral, $(n - 1)$ is the refractivity and is normally given in parts-per-million i.e., $(n - 1) = 10^{-6}N$. For optical frequencies, the refractivity, *N*, is given by [*Owens*, 1967]

$$N = k_1(\lambda)\frac{P_d}{T}Z_d^{-1} + k_2(\lambda)\frac{P_w}{T}Z_w^{-1} \tag{1.3}$$

where $k_1(\lambda)$ and $k_2(\lambda)$ are experimentally determined functions of the laser wavelength, λ, which relate the refractivity to the molecular density of the dry-air constituents of the atmosphere and to the density of water vapor. P_d and P_w are the partial pressures of dry-air and water vapor, T is temperature, and Z_d and Z_w are the compressibilities of dry-air and water vapor. The compressibilities enter through the non-ideal gas law in the form

$$\rho_i = \frac{P_i}{T}\frac{M_i}{R}Z_i^{-1} \tag{1.4}$$

where ρ_i is the density of gas i (dry air or water vapor in the case of the atmosphere) with molecular weight M_i and compressibility Z_i, at pressure P_i and temperature T; and R is the Universal gas constant. For reasons that will become clearly shortly, Equation (1.3) is often combined with Equation (1.4) and written such that the total density of gas, $\rho = \rho_d + \rho_w$, appears. In this form Equation (1.3) becomes

$$N = k_1\frac{R}{M_d}\rho + \left(k_2 - k_1\frac{M_w}{M_d}\right)\frac{R}{M_w}\rho_w \tag{1.5}$$

where we have dropped the dependence of k_1 and k_2 on wavelength for simplicity. The reason for this choice of form for refractivity is that the first term is the largest term and with the assumptions that the atmosphere is in hydrostatic equilibrium and gravity is constant through the atmospheric column, the integral in Equation (1.2) for the range correction can be solved exactly. To obtain this form, we use the hydrostatic equation

$$\frac{dP}{dz} = -\rho(z)g(z) \tag{1.6}$$

where $\frac{dP}{dz}$ is the height derivative of pressure as a function of height z and $g(z)$ is the gravitational acceleration. Substituting Equation (1.6) into the first term of Equation (1.5) and then substituting into Equation (1.2) yields the "hydrostatic" component of the range correction, ΔL_H, which can be written as

$$\Delta L_H = 10^{-6} k_1 \frac{R}{M_d} g_m^{-1} \int_Z^{\infty} \frac{dP}{dz} dz \tag{1.7}$$

where g_m is the mean value of gravity in the column of the atmosphere. Since gravity decreases slowly with height and can be closely approximated with a simple function of latitude, this value can be expressed accurately in terms of the height, *Z*, and latitude, ϕ, of the ground point to which the altimeter measurement is made [*Saastamoinen*, 1972]

$$g_m = 9.8062(1 - 0.00265\cos(2\phi) - 3.1\times10^{-7}(0.9Z + 7300)) \ \text{ms}^{-2} \tag{1.8}$$

Equation (1.7) can be further reduced because the integral is simply the surface pressure at height *Z*, and therefore the largest part of the atmospheric range correction in the zenith direction is given by

$$\Delta L_H = 10^{-6} k_1 \frac{R}{M_d} g_m^{-1} P_{SURF} \tag{1.9}$$

where P_{SURF} is the surface pressure.

The remaining part of the zenith atmosphere range correction is due to the residual part of the water vapor not included in the hydrostatic term, sometimes called the "wet" component, ΔL_W. Substituting the second term of Equation (1.5) into equation (1.2) gives

$$\Delta L_W = 10^{-6} k_2' \frac{R}{M_w} \int_Z^{\infty} \rho_w dz \tag{1.10}$$

where $k_2' = k_2 - k_1 \frac{M_w}{M_d}$. The integral is simply the total column precipitable water vapor, *PW*, an atmospheric variable often reported in atmospheric models. The zenith wet delay can now be written as

$$\Delta L_W = 10^{-6} k_2' \frac{R}{M_w} PW \tag{1.11}$$

The empirical functions in the refractivity equation are given by Owens [1967] as

$$k_1 = 0.237134 + 68.39397 \frac{(130 + \lambda^{-2})}{(130 - \lambda^{-2})^2} + 0.45473 \frac{(38.9 + \lambda^{-2})}{(38.9 - \lambda^{-2})^2} \tag{1.12}$$

$$k_2 = 0.648731 + 0.0174174\lambda^{-2} + 3.55750\times10^{-4}\lambda^{-4} + 6.1957\times10^{-5}\lambda^{-6} \quad (1.13)$$

where λ is in μm. For the GLAS laser wavelength of 1.064 μm, $k_1 = 0.78661\,\mathrm{K/Pa}$ and $k_2 = 0.66444\,\mathrm{K/Pa}$. Given molecular weights of dry air and water vapor of M_d = 28.9644 kg kmol^{-1} and M_w = 18.0152 kg kmol^{-1}, respectively, $k_2' = 0.17519\,\mathrm{K/Pa}$. Combining these values into Equations (1.9) and (1.11) gives the final zenith delay equations

$$\Delta L_Z = \Delta L_H + \Delta L_W \quad (1.14)$$

$$\begin{aligned} \Delta L_H &= (2.258\,\mathrm{m^2 s^2/Pa}) g_m^{-1} P_{SURF} \\ &\approx (2.302\times10^{-5}\,\mathrm{m/Pa}) P_{SURF} \end{aligned} \quad (1.15)$$

$$\text{for } g_m(90^o, 0) = 9.8100\,\mathrm{ms^{-2}}$$

$$\Delta L_W = (8.085\times10^{-5}\,\mathrm{m/(kg/m^2)}) PW \quad (1.16)$$

Given an average surface pressure value of 10^5 Pa, the zenith hydrostatic delay is approximately 2.35 m and is the major component of total delay. Zenith wet delay is much more variable, given precipitable water vapor values of less than 10 mm in the polar regions to 50 mm in the tropics, the corresponding zenith wet delay varies from 1 to 4 mm.

2.2 Mapping Function

The mapping function relates the total atmospheric delay at an arbitrary elevation angle to the zenith delay such that

$$\Delta L = m(\varepsilon, \boldsymbol{P}) \Delta L_Z \quad (2.1)$$

When it is assumed that the refractivity of the troposphere is spherically symmetric, Marini [1972] showed that the continued fraction form of the mapping function is

$$m(\varepsilon) = \cfrac{1}{\sin\varepsilon + \cfrac{a}{\sin\varepsilon + \cfrac{b}{\sin\varepsilon + \cfrac{c}{\sin\varepsilon + \ldots}}}} \quad (2.2)$$

where a, b, c, ... are parameters that may be approximated using climatic data. The very simplest form of this equation is

$$m(\varepsilon) = \frac{1}{\sin\varepsilon} \tag{2.3}$$

A number of different forms of the mapping function have been published, we will compare Equation (2.3) to two different but widely using mapping functions. One is by Davis, et al [1985], named CfA-2.2, which depends on surface pressure and surface temperature. The other by Niell [1996] which depends on latitude and day of year. The different climatic variables used are due to the different climatologies and functional forms of the parameters used. We compared the simple mapping function to the test functions by subtracting the test function from the simple mapping function and multiplying by 2.3 m, which is a typical value for zenith delay. This comparison gives estimates of how much the total delay will change when different mapping functions are used.

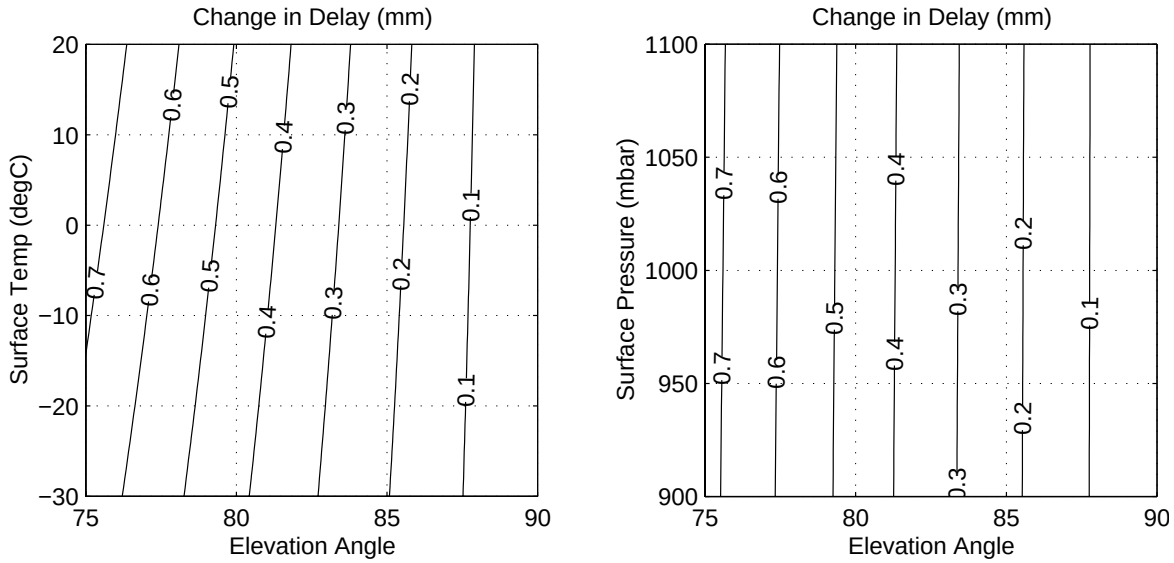

Figure 1. Change in delay of the simple mapping function compared to CfA-2.2 mapping func-

tion. Left plot is for P_0 = 1000 mbar, right plot is for T_0 = 0°C.

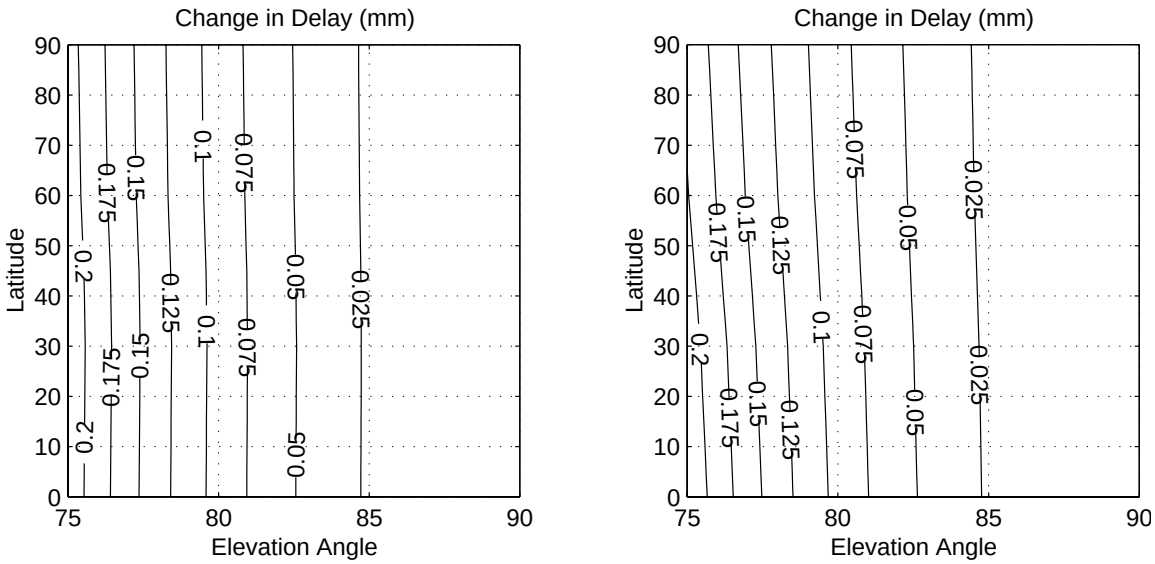

Figure 2. Change in delay of the simple function compared to Niell mapping function. Left plot is for maximum day of year phase, right plot is for minimum day of year phase.

For both of the comparisons, using the simple form of the mapping functions compares very closely to the other forms. We don't expect that the GLAS space craft will point beyond 10° off nadir, the differences in this region are less than 0.5 mm for CfA-2.2 and 0.1 mm for Niell. It should be noted that these other mapping functions are optimized for low elevation angles and in fact we expect the Niell mapping function to be more accurate at higher elevation angles due to its functional form. So we will use the simple $m(\varepsilon) = 1/(\sin\varepsilon)$ form of the mapping function.

Another concern for off-nadir pointing of the space craft is the change in footprint location due to bending of the ray in the atmosphere. This effect will not significantly change the atmospheric delay calculation but should be considered for space craft pointing calibrations where the location

of the laser footprint is directly measured at the ground.

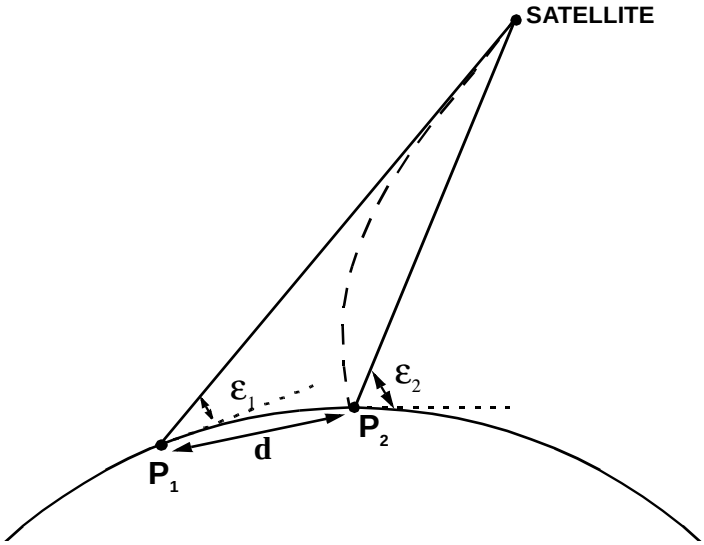

Figure 3. Geometry of laser ray path.

The real curved path is shown by the dashed line in Figure 3. P_1 is the expected ground location of the laser footprint for the satellite position and pointing angle, $\alpha_1 = 90° - \varepsilon_1$, as measured at the satellite. P_2 is the real ground location of the laser footprint after following the refracted path through the atmosphere, which is shifted by a distance d towards the sub-satellite point. If the satellite position and real footprint location were used to calculate the apparent satellite pointing angle, $\alpha_2 = 90° - \varepsilon_2$, this would be in error by a certain amount such that $\alpha_1 = \alpha_2 - \delta\alpha$. This correction can be approximated by a simple expression for pointing angles of less than 75° [*Astronomical Almanac,* 1999] such that

$$\delta\alpha = 0.00452° P \tan\alpha_2 / (273 + T) \tag{2.4}$$

where T is the temperature (°C) and P is the pressure (mbar) at the surface. Using NOAA mean values of 15°C and 1013 mbar, Equation (2.4) gives an approximate value of

$$\begin{aligned} \delta\alpha &= 0.016° \tan\alpha_2 \\ &= 57'' \tan\alpha_2 \end{aligned} \tag{2.5}$$

At an altitude of 600 km and pointing angle of 10 degrees, the pointing error will be approximately 10 arcseconds and the distance the laser footprint is shifted by will be 30 m.

This correction equation may also be used to estimate whether horizontal gradients in the pressure fields will greatly affect the path of the laser pulse. A typical upper value of the synoptic pressure gradient is 10 mbar per 100 km. Near the surface the derivative of pressure with respect to height is approximately 0.1 mbar/m. This means that a typical slope to the pressure field is 0.05 degrees.

Assuming that this gradient is constant through the atmosphere (actually, should decrease exponentially) we can put this angle into Equation (2.5) to see how much the path will deviate. For a 0.05 degree slope the deviation is 0.06 arcseconds which corresponds to a 15 cm shift in the footprint location. This amount of ray deviation will have no discernable effect of the atmospheric delay.

2.3 External Data

We require a data set that will allow us to calculate values for surface pressure and total precipitable water vapor at the laser footprint locations. The data will we use are the National Center for Environmental Prediction (NCEP) global analyses. These are produced by NCEP as a routine operational analysis and can be downloaded near real time at an anonymous NOAA ftp site, ftp.ncep.noaa.gov. A further guide to using this ftp site can be found in an on-line reference by Quinn [1999]. Data sources include ground stations, radiosondes, satellites, and buoys. The global analyses are produced on 1 degree grid uniform and complete in latitude and longitude, with a sampling rate of 6 hours, starting at 0 GMT. These analyses consist of many meteorological variables for a range of levels from the surface to the stratosphere. The variables that we will use for our surface pressure model are temperature, geopotential height, and relative humidity for the tropospheric pressure levels between 1000 mbar and 300 mbar. The total precipitable water vapor is given as a single field integrated through the entire atmospheric column. The NCEP global analyses are described in more detail in an on-line reference by Huang [1995].

The NCEP analyses also have a surface pressure field, produced from unreduced station pressures. This field is decidedly unsatisfactory over rapid changes in elevation. The relatively flat surfaces adjacent to steep gradients show an artifact called Gibbs effect, which is a ripple in the pressure field where there should be none. This is caused by the spectral method used to interpolate this field, which is why we need a more reliable surface pressure model that utilizes the upper atmospheric fields.

2.4 Surface Pressure Model

An atmospheric model of pressure with respect to height is required to reduce the upper level NCEP fields to a surface pressure. To simplify the physical model of the atmosphere we will make certain assumptions. A static atmosphere model will allow us to consider the vertical distribution of atmospheric variables. Although the atmosphere is actually a dynamic system, static atmosphere formulas for variables like pressure and density are valid to a high degree of accuracy. We will assume a horizontally stratified atmosphere in hydrostatic equilibrium, such that pressure is related to height by the hydrostatic equation

$$dP = -g(Z)\rho(Z)dZ \tag{4.1}$$

where Z is geometric height, P is pressure, g is gravity, and ρ is density.

To allow easier integration of this equation, we will convert geometric height into geopotential height. A geopotential meter is defined as the work done by lifting a unit mass one geometric meter through a region in which gravity is uniformly 9.80665 m/s^2, the value of mean sea level gravity. The geopotential measured with respect to mean sea level (assumed zero potential) is

called geopotential height, *H*, such that

$$H = \frac{1}{g_0}\int_0^Z g\,dz \tag{4.2}$$

where g_0 = 9.80665 m^2/s^{2}m' [*NOAA*, 1976]. The derivative of this equation with respect to geometric height is

$$g_0 dH = g\,dZ \tag{4.3}$$

This can be substituted into the hydrostatic equation to give

$$dP = -g_0 \rho(H)\,dH \tag{4.4}$$

We now require an expression that will convert elevation in geometric meters to geopotential meters. This will be related to the variation of gravity with height. Approximating the Earth as a sphere with only radial mass variations, gravity is inversely proportional to radius squared, which will give a conversion equation of

$$g = g_{msl}\left(1 + \frac{2Z}{R_e}\right) \tag{4.5}$$

where R_e = 6378077m is radius of Earth, g_{msl} is gravity at mean sea level. Substituting this equation for gravity into Equation (4.5) gives the conversion formula

$$H = \frac{g_{msl}}{g_0} Z\left(1 - \frac{Z}{R_e}\right) \tag{4.6}$$

Mean sea level gravity depends on geodetic latitude, the formula is based on calculations of the standard reference ellipsoid [*Emerson & Wilkins*, 1971] such that

$$g_{msl} = g_{eq}(1 + k\sin^2\phi)(1 - e^2\sin^2\phi)^{-\frac{1}{2}} \tag{4.7}$$

where ϕ is latitude, g_{eq} = 9.7803184558 m/s^2, k = 0.00193166338321, e = 0.00669460532856.

Many atmospheric models, such as the U.S. Standard Atmosphere [*NOAA*, 1976], simplify their calculations for pressure by assuming the air to be a dry, ideal gas. We shall include non-ideal gas effects and water vapor partial pressure. The equation of state for a pure non-ideal gas is

$$Z^{-1}\frac{PV}{RT} = \frac{m}{M} \tag{4.8}$$

where Z^{-1} is called the inverse compressibility and depends empirically on pressure and temperature [*Harrison,* 1965b], P is pressure, V is volume, R is the universal gas constant, T is temperature, m is mass, and M is molecular weight.

Density can be written as $\rho = m / V$, and we can split mass components of water and dry air: $m = m_w + m_d$. If we assume that moist air obeys Dalton's Law of partial pressures, the separate masses can be evaluated by the non-ideal equation of state to give a density equation of

$$\rho = \frac{1}{RT}(Z_w^{-1} P_w M_w + Z_d^{-1}(P - P_d) M_d) \tag{4.9}$$

where R = 8314.510 J/kmol.K, M_w = 18.01534 kg/kmol, M_d = 28.9645 kg/kmol, P is the total pressure and P_w is the partial pressure of the water vapor in the air. It is implicitly assumed that the dry air components are homogeneously mixed throughout the lower atmosphere and therefore the mean molecular weight of dry air is a constant [*NOAA,* 1976].

Equations for inverse compressibility have been experimentally determined by Owens [1967], these formulas are accurate to within a few parts per million

$$\begin{aligned} Z_w^{-1} = 1 + 1650\frac{P_w}{T^3}[1 - 0.01317(T - 273.15) \\ \ldots + 1.75\times10^{-4}(T - 273.15)^2 \\ \ldots + 1.44\times10^{-6}(T - 273.15)^3] \end{aligned} \tag{4.10}$$

$$\begin{aligned} Z_d^{-1} = 1 + (P - P_w)\left[57.90\times10^{-8}\left(1 + \frac{0.52}{T}\right)\right. \\ \left. \ldots - 9.4611\times10^{-4}\frac{(T - 273.15)}{T^2}\right] \end{aligned} \tag{4.11}$$

We need an equation for water vapor pressure. Water vapor pressure is related to the saturation vapor pressure using relative humidity [*Harrison,* 1965a]:

$$P_w = RhP_s \tag{4.12}$$

where relative humidity is in a fractional form with values between 0 and 1. This equation is only true for pure water vapor, *not* moist air. However the equation is approximately true for moist air. The World Meteorological Organization (WMO) has adopted the practice of evaluating relative humidity with respect to liquid water at all temperatures, even those below 0 °C.

Saturation vapor pressure is often expressed as a sum of analytical basic functions with empirically determined weight. One of the better forms uses Chebyshev polynomials [*McGarry,* 1983]

$$T\log_{10}\left(\frac{P_s}{P_b}\right) = \frac{a_o}{2} + \sum_{s=1}^{n} a_s E_s(x) \tag{4.13}$$

where P_b = 1000 Pa, P_s is saturation vapor pressure, $E_s(x)$ are Chebyshev polynomials:

$$\begin{aligned} E_0(x) &= 1 \\ E_1(x) &= x \\ E_{s+1}(x) &= 2xE_s(x) - E_{s-1}(x) \\ x &= \frac{2T - (T_{max} + T_{min})}{T_{max} - T_{min}} \end{aligned} \tag{4.14}$$

The coefficients a_s (s = 0,...,10) are a_s = {2794.027, 1430.604, -18.234, 7.674, -0.022, 0.263, 0.146, 0.055, 0.033, 0.015, 0.013}, T_{max} = 648 K, and T_{min} = 273 K [*Ambrose*, 1987].

We now have an expression for density that depends on temperature, relative humidity and pressure. To solve the hydrostatic equation we must express temperature and relative humidity as functions of geopotential height, in order to get an expression for density that only depends on geopotential height. The NCEP global analyses have values for temperature, geopotential height and relative humidity at standard pressure levels. We shall assume that temperature varies linearly with respect to geopotential height between these levels, a relatively good assumption for the lower atmosphere such that

$$T = T_0 + L(H - H_0) \tag{4.15}$$

$$L = \frac{T_1 - T_0}{H_1 - H_0} \tag{4.16}$$

where L is the temperature gradient; T_0 and H_0 are temperature and geopotential height at the upper level; T_1 and H_1 are temperature and geopotential height at the lower level: $H_1 < H \leq H_0$. We will also assume that relative humidity varies linearly with respect to geopotential height between levels such that

$$Rh = Rh_0 + S(H - H_0) \tag{4.17}$$

$$S = \frac{Rh_1 - Rh_0}{H_1 - H_0} \tag{4.18}$$

where S is the relative humidity gradient, Rh_0 is relative humidity at the upper level, Rh_1 is relative humidity at the lower level. Given these expressions for temperature and relative humidity, the hydrostatic equation becomes

$$\frac{dP}{dH} = -\frac{g_0}{RT(H)}[Z_v^{-1}(H)P_v(H)M_v + Z_a^{-1}(H, P)[P - P_v(H)]M_a] \quad (4.19)$$

This differential equation is first order, non-linear and inhomogeneous, we are not able find an analytic solution. To obtain a numerical solution for pressure we will numerically integrate down from the upper level geopotential height to the desired geopotential height. Pressure varies smoothly with geopotential height, this means that we are relatively unrestricted in our choice of numerical method. We will use the Bulirsch-Stoer method, which is one of the best ways to obtain high accuracy solutions with minimal computational effort, provided the integrated function is smooth and has no singular points within the range of integration [*Press et al*., 1989].

2.5 Precipitable Water Vapor

The NCEP global analyses give total column precipitable water vapor as a single field evaluated at the surface, we will use this without modification as input into the zenith wet delay equation. The precipitable water vapor contribution to total delay is small but highly variable both spatially and temporally and should be monitored throughout the ICESat mission. Unfortunately, the global analyses are less accurate in the polar regions, especially in the southern regions where there is a scarcity of data. The NCEP water vapor fields are particularly troublesome.

To validate the precipitable water vapor fields we will compare them to ground station data. One of resources we will use is the GPS global network [*Quinn & Herring*, 1999]. Precipitable water vapor can be derived from estimates of GPS tropospheric delay made at each global station. This derivation requires the knowledge of surface pressure at the station. There are over 35 GPS stations that report surface pressure from on site met packages, however only two of these are in the polar regions, both in the north. Where directly measured surface pressure is unavailable we can use our own surface pressure model without a significant loss of accuracy. There are currently 4 stations in Antarctica and 6 stations in the Arctic where we can make precipitable water vapor measurements. The major advantage of using the GPS global network is the rapid availability of data and confidence that the data will be available over the length of the ICESat mission.

2.6 Delay Correction with Respect to Height

As can be seen in the previous sections, calculation of surface pressure and therefore delay requires a knowledge of the height of the laser footprint location. The atmospheric delay correction will be performed early in the GLAS processing and there may be later adjustments to the space craft orbit and footprint location height. We wish to have a simple correction function that would be accurate for changes in height of ±100 m.

The simplest case, case (a), would be to assume that *dP/dH* is a constant with respect to height, this would imply a linear correction function such that

$$\begin{aligned} P &= P_0(1 - A(H - H_0)) \\ A &= \frac{g_0 Z_d^{-1} M_d}{RT_0} \end{aligned} \quad (6.1)$$

where P and H are the corrected pressure and geopotential height, P_0 and H_0 are the original pressure and geopotential height. The next simplest case, case (b), would be to assume that dP/dH is proportional to P and temperature is constant with respect to height. These assumptions lead to an exponential correction function such that

$$\begin{aligned} P &= P_0 e^{(-A(H - H_0))} \\ A &= \frac{g_0 Z_d^{-1} M_d}{R T_0} \end{aligned} \tag{6.2}$$

The most accurate case, case (c), assumes that temperature is linearly dependant on height and dP/dH is proportional to P/T. These assumptions lead to a power law correction function such that

$$\begin{aligned} P &= P_0 \left(\frac{T}{T_0} \right)^{-B} \\ B &= \frac{g_0 Z_d^{-1} M_d}{L R} \\ T &= T_0 + L(H - H_0) \end{aligned} \tag{6.3}$$

All three case assume that water vapor is negligible and that the inverse compressibility does not change with respect to height.

To compare these three cases, we can use average values for the variables of $P_0 = 10^5$ Pa, $T_0 = 273$ K, $L = -0.0065$ K/m, and $g_0 Z_d^{-1} M_d / R = 0.034$ K/m. For a change in height of 100 m, case (a) gives a change in pressure of -1251.4 Pa, case (b) gives -1243.6 Pa, and case (c) gives 1245.1 Pa. We would like to use the most accurate equation, however we must consider the storage costs of each case. Case (a) and (b) require that the one correction parameter, A, be saved in the geophysical record. Case (c) requires that three correction parameters, B, T_0, and L, be saved. The difference between (b) and (c) is only 1.5 Pa, whereas the difference between (a) and (c) is 6.3 Pa. For no extra storage cost we can use the more accurate correction equation given Equation (6.2) and recover better than 99.9% of the change in pressure for height changes of less than 100 m.

Since atmospheric delay is approximately proportional to surface pressure, again neglecting water vapor, the correction equation may be directly applied such that

$$\begin{aligned} \Delta L &= \Delta L_0 e^{(-A(H - H_0))} \\ A &= \frac{g_0 Z_d^{-1} M_d}{R T_0} \end{aligned} \tag{6.4}$$

2.7 Spatial Interpolation

The NCEP global analyses we will use are given on a 1 by 1 degree uniform latitude and longitude grid. We require an interpolation scheme that will allow us calculate the atmospheric field values at the laser footprint locations. This interpolation method will have to be computationally efficient to keep up with the real time data processing requirements. The global analyses have the highest realistic spatial resolution by design, therefore a complicated interpolation scheme intended for sparse data sets would not be useful nor appropriate. The upper level fields of temperature, geopotential height and relative humidity are quite smooth, a bilinear interpolation of the grid will be sufficient. The precipitable water vapor field is much more variable, however its accuracy and small contribution to the total delay do not warrant anything more complicated than bilinear interpolation as well.

Bilinear interpolation has the form

$$\begin{aligned} f(\phi, \lambda) &= a + bX + cY + dXY \\ a &= f(\phi_1, \lambda_1) \\ b &= f(\phi_1, \lambda_2) - f(\phi_1, \lambda_1) \\ c &= f(\phi_2, \lambda_1) - f(\phi_1, \lambda_1) \\ d &= f(\phi_1, \lambda_1) + f(\phi_2, \lambda_2) - f(\phi_1, \lambda_2) - f(\phi_2, \lambda_1) \\ X &= (\lambda - \lambda_1) / (\lambda_2 - \lambda_1) \\ Y &= (\phi - \phi_1) / (\phi_2 - \phi_1) \end{aligned} \tag{7.1}$$

where f is the field value, ϕ is latitude, λ is longitude. The subscripts 1 and 2 stand for south and north latitudes and the west and east longitudes of the four known grid points directly surrounding the unknown point.

2.8 Temporal Interpolation

Analysis of the power spectra of surface pressure changes has shown that these spectra fall off at high frequencies with an approximate f^{-2} frequency dependence [*Quinn*, 1996]. This type of spectral behavior is consistent with a random walk stochastic process. For these processes, the maximum likelihood interpolator is simply a linear interpolation between adjacent points. The current NCEP global analyses are sampled every 6 hours and the integrated power in the power spectra for periods of less than 6 hours, as calculated from higher resolution ground station data, indicates that linear interpolation should yield pressure estimates with errors less than 1 mbar. This corresponds to total delay errors of less than 2.35 mm.

3.0 References

Ambrose, D., Pressure-volume-temperature, in *Recommended Reference Materials for the Realization of Physiochemical Properties*, K. N. Marsh ed., Blackwell Sci. Pub., 73-114, 1987.

Astronomical Almanac, U. S. Government Printing Office, 1999.

Davis, J. L., T. A. Herring, I. I. Shapiro, A. E. E. Rogers and G. Elgered, Geodesy by radio interferometry: Effects of atmospheric modeling errors on estimates of baseline length, *Radio Sci., 20,* 1593-1607, 1985.

Dongarra, J. J. *et al.*, LINPACK User's Guide, SIAM, Philadelphia, 1979.

Emerson, B. and G. A. Wilkins, The IAU system of astronomical constants, *Celes. Mech., 4*, 142, 1971.

Harrison, L. P., Fundamental concepts and definitions relating to humidity, in *Humidity and Moisture*, A. Wexler ed, Reinhold Pub. Co., New York, vol. 3, 3-70, 1965.

Harrison, L. P., Imperfect gas relationships, in *Humidity and Moisture*, A. Wexler ed, Reinhold Pub. Co., New York, vol. 3, 3-70, 1965.

Huang, F., Description of selected products from the NOAA NCEP gridded data, *http://spsosun.gsfc.nasa.gov/nmc_rev4.html*, 1995

Marini, J. W., Correction of satellite tracking data for an arbitrary tropospheric profile, *Radio Sci., 7*, 223-231, 1972.

McGarry, J., Correlation and Prediction of the Vapor Pressures of Pure Liquids over Large Pressure Ranges, *Ind. Eng. Chem. Process Des. Dev., 22*, 313-322, 1983.

National Oceanic and Atmospheric Administration, U.S. Standard Atmosphere, 1976.

Niell, A. E., Global mapping functions for the atmospheric delay at radio wavelengths, *J. Geophys. Res., 101(B2)*, 3227-3246, 1996.

Owens, J. C., Optical refractive index of air: Dependence on pressure, temperature, and composition, *Appl. Opt., 6,* 51-59, 1967.

Press, W. H., B. P. Flannery, S. A. Teukolsky, W. T. Vetterling, Numerical Recipes, Cambridge Uni. Press, 1989.

Quinn, K. J., Annual report of the GLAS tropospheric delay science team, 1996.

Quinn, K. J. and T. A. Herring, Using the global GPS network to validate atmospheric delay corrections to the ICESat laser altimeter ranges, *EOS Trans. AGU, 79 Suppl.,* 200, 1999.

Quinn, K. J., Meteorological Data Guide for Geodesists, *http://www-gpsg.mit.edu/~katyq/gpsmet/gpsmet_primer.html*, 1999.

Saastamoinen, J., Atmospheric correction for the troposphere and stratosphere in radio ranging of satellites, in *The Use of Artificial Satellites for Geodesy, Geophys. Monogr. Ser., vol. 15*, edited by S. W. Henriksen, A. Mancini, and B. H. Chovitz, 247-251, AGU, Washington D. C., 1972.